Clin Kidney J (2012) 5: 535–544
doi: 10.1093/ckj/sfs140
Advance Access publication 7 November 2012

Clinical Research

CKJ

Increased expression of renal TRPM6 compensates for Mg^{2+} wasting during furosemide treatment

Annelies A. van Angelen, AnneMiete W. van der Kemp, Joost G. Hoenderop and René J. Bindels

Department of Physiology, Radboud University Nijmegen Medical Centre, Nijmegen, the Netherlands

Correspondence and offprint requests to: René J Bindels; E-mail r.bindels@fysiol.umcn.nl

Abstract

Background. Furosemide is a loop diuretic, which blocks the Na^+, K^+, $2Cl^-$ cotransporter (NKCC2) in the thick ascending limb of Henle (TAL). By diminishing sodium (Na^+) reabsorption, loop diuretics reduce the lumen-positive transepithelial voltage and consequently diminish paracellular transport of magnesium (Mg^{2+}) and calcium (Ca^{2+}) in TAL. Indeed, furosemide promotes urinary Mg^{2+} excretion; however, it is unclear whether this leads, especially during prolonged treatment, to hypomagnesaemia. The aim of the present study was, therefore, to determine the effect of chronic furosemide application on renal Mg^{2+} handling in mice.

Methods. Two groups of 10 mice received an osmotic minipump subcutaneously for 7 days with vehicle or 30 mg/kg/day furosemide. Serum and urine electrolyte concentrations were determined. Next, renal mRNA levels of the epithelial Mg^{2+} channel (TRPM6), the Na^+, Cl^- cotransporter (NCC), the epithelial Ca^{2+} channel (TRPV5), the cytosolic Ca^{2+}-binding protein calbindin-D_{28K}, as well parvalbumin (PV), claudin-7 (CLDN7) and claudin-8 (CLDN8), the epithelial Na^+ channel (ENaC) and the Na^+–H^+ exchanger 3 (NHE3) were determined by real-time quantitative polymerase chain reaction. Renal protein levels of NCC, TRPV5, calbindin-D_{28K} and ENaC were also measured using semi-quantitative immunohistochemistry and immunoblotting.

Results. The mice chronically treated with 30 mg/kg/day furosemide displayed a significant polyuria (2.1 ± 0.3 and 1.3 ± 0.2 mL/24 h, furosemide versus control respectively, $P < 0.05$). Furosemide treatment resulted in increased serum concentrations of Na^+ [158 ± 3 (treated) and 147 ± 1 mmol/L (control), $P < 0.01$], whereas serum K^+, Ca^{2+} and Mg^{2+} values were not significantly altered in mice treated with furosemide. Urinary excretion of Na^+, K^+, Ca^{2+} and Mg^{2+} was not affected by chronic furosemide treatment. The present study shows specific renal upregulation of TRPM6, NCC, TRPV5 and calbindin-D_{28K}.

Conclusions. During chronic furosemide treatment, enhanced active reabsorption of Mg^{2+} via the epithelial channel TRPM6 in DCT compensates for the reduced reabsorption of Mg^{2+} in TAL.

Keywords: DCT; furosemide; mouse; polyuria; TRPM6

Introduction

Furosemide is a loop diuretic, which blocks the Na^+, K^+, $2Cl^-$ cotransporter (NKCC2) in the thick ascending limb of Henle (TAL) [1] by competing for the chloride site on the transporter [2]. Interestingly, most magnesium (Mg^{2+}) reabsorption takes place in TAL (~60%) in a passive, paracellular way [3, 4]. This reabsorption is driven by the transepithelial potential mediated by transport via NKCC2. Furosemide treatment is usually prescribed primarily for its natriuretic action as treatment of edematous status and hypertension [5]. By diminishing sodium (Na^+) reabsorption, the concentrating process that occurs in the renal medulla is impaired and fluid loss ensues. On the short term, this results in diminished Na^+ and chloride (Cl^-) reabsorption, and as a consequence, due to increased distal Na^+ delivery and increased levels of aldosterone, potassium (K^+) loss. In TAL, the generation of a lumen-positive transepithelial voltage by NKCC2 is diminished by treatment with furosemide, consequently paracellular transport of Mg^{2+} and calcium (Ca^{2+}) is reduced resulting in increased urinary excretion of these ions [6–8]. Chronic effects of furosemide treatment sometimes result in hypercalciuria, but only rarely lead to hypocalcaemia [9, 10]. Long-term effects of treatment with furosemide on urinary and serum Mg^{2+} values vary, in such a way that hypomagnesaemia is sometimes observed in patients with heart failure or other serious diseases; a disorder not generally observed in patients with sufficient Mg^{2+} intake and no disturbance in Mg^{2+} balance [9, 11, 12]. However, data of chronic furosemide treatment in healthy volunteers or animal models are scarce and seem to lack analysis of Mg^{2+} homeostasis in relation to other electrolytes.

A complicating factor of chronic furosemide use is the development of resistance, which decreases the long-term efficacy [13]. On the one hand, decreased efficacy with time occurs because of the 'braking phenomenon' [14]. This phenomenon is the result of adaptation in the distal convoluted tubule (DCT) and connecting tubule (CNT), due to the chronically increased Na^+ delivery to these nephron segments [15–17]. On the other hand, resistance develops due to the short-acting characteristic of furosemide, with a peak plasma concentration after ~1 h of furosemide treatment [18, 19]. Thus, increased reabsorption of Na^+ can be observed rapidly, know as the 'rebound phase' [14]. As an indicator of resistance to chronic furosemide treatment, particularly the impaired natriuretic response was determined by measuring renal Na^+ excretion levels [15]. It is interesting to unravel if the excretion of in particular Mg^{2+} is affected similarly. Like the clinical implications for furosemide use, hypomagnesaemia is only sporadically observed in antenatal Bartter syndrome [20]. This disorder is caused by mutations in genes facilitating transcellular NaCl reabsorption in TAL, including the gene encoding NKCC2 (*SLC12AI*). This hereditary recessive disease, which impairs the transport function of the TAL, is characterized by prenatal onset, a severe salt-wasting state with low blood pressure, hypokalemic metabolic alkalosis, hyperreninaemia, polyuria, hyperprostaglandinuria and often hypercalciuria [21].

The aim of the present study was to unravel whether chronic furosemide treatment leads to hypomagnesaemia or that other parts of the nephron can compensate for the reduced Mg^{2+} reabsorption in TAL. For this purpose, the chronic effect of furosemide on renal handling of Mg^{2+} was studied in mice. The fine-tuning of Mg^{2+} excretion is mediated by the early DCT (DCT1), where active transcellular reabsorption takes place via the epithelial Mg^{2+} channel (TRPM6) [22]. Therefore, the expression level of TRPM6 was measured as well as the level of the Na^+, Cl^- cotransporter (NCC). This protein is, like TRPM6, expressed exclusively along the apical membrane of the DCT [23].

Subjects and methods

Animal studies

Male C57BL/6J mice (10 weeks of age) were purchased from Harlan/CPB (Zeist, The Netherlands) and roomed in a temperature- and light-controlled room with *ad libitum* access to standard pellet chow (0.19% w/w Mg^{2+}, SSNIFF Spezialdiäten GmbH, Soest, Germany) and drinking water. Mice were randomly assigned to either the control or furosemide treatment group (10 per group). Furosemide (Sigma, St Louis, MO, USA) was administered using osmotic minipumps (Alzet, Cupertino, CA, USA) subcutaneously for 7 days with vehicle or 30 mg/kg/day furosemide. Before and after the treatment, the mice were individually housed in metabolic cages enabling 24 h urine collections under mineral oil (to prevent evaporation) and to measure their water and food intake. At the end of the experiment, blood samples were taken under isoflurane anaesthesia and the mice were sacrificed. Subsequently, kidneys were frozen immediately in liquid nitrogen or incubated in periodate–lysine–paraformaldehyde (PLP) solution for RNA isolation, immunoblotting and immunohistochemistry (IHC) analysis, respectively. Blood was led to clot at room temperature, incubated overnight at 4°C and spun down for 5 min at 13 250 × *g*, and the collected serum was subsequently used for analytical procedures. The animal ethics board of the Radboud University Nijmegen approved all experimental procedures.

Analytical procedures

Serum Mg^{2+} concentration and urinary Mg^{2+} excretion were determined using a colorimetric assay kit according to the manufacturer's protocol (Roche Diagnostics, Woerden, the Netherlands). Serum and urine Ca^{2+} concentrations were measured colorimetrically as described previously [24]. A flame spectrophotometer (FCM 6343; Eppendorf) was used to measure serum and urine Na^+ and K^+ concentrations.

Total kidney RNA isolation and cDNA synthesis

Total RNA was extracted from the kidney using TriZol Total RNA Isolation Reagent according to standard procedures (Gibco BRL, Breda, the Netherlands). The obtained RNA was subjected to DNase treatment (Promega, Madison, WI, USA) to prevent genomic DNA contamination. All samples were resolved on 1% w/v formaldehyde agarose gel to evaluate the RNA quality, while RNA concentration was determined by measuring the ratio of the UV absorbance at 260 and 280 nm using the NANODROP 2000c (Thermo Scientific, Wilmington, DE, USA). Thereafter, 1.5 µg of RNA was reverse transcribed by Molony-Murine Leukaemia Virus-Reverse Transcriptase (MMLV-RT) (Invitrogen, Breda, The Netherlands) into cDNA according to the manufactures recommendations.

SYBR Green real-time quantitative polymerase chain reaction

The cDNA was used to determine the mRNA expression levels of genes of interest, as well as mRNA levels of the reference gene glyceraldehyde 3-phosphate dehydrogenase (GAPDH) as an endogenous control. Primer3 software (http://frodo.wi.mit.edu/primer3/) was used to design real-time polymerase chain reaction (PCR) primers according to the general criteria for real-time-primers. All primer sets were intron-overspanning, except for *CLDN8*, because this gene consists of only one exon. All primer sequences used in this study are listed in Table 1. Prior to real-time PCR, the efficiency (95–105%) and dynamic range ($R^2 > 0.98$) were evaluated for each primer set. Real-time PCRs were performed on a Biorad CFX96™. Real-time PCR and Biorad C1000™ Thermal Cycler system. Reactions were performed in duplo using 6.25 µL of SYBR®-Green Master Mix (Applied Biosystems, Foster City, CA, USA), 12.5 ng of template cDNA and 400 nM each primer in a final volume of 12.5 µL. All amplicons showed the correct sizes after gel electrophoresis and the dissociation curves showed one distinct melting peak, ensuring the absence of a non-specific byproduct or primer dimers. Moreover, no reverse transcription controls and no template controls were taken, and the difference between the samples was at least eight ct-values, but most of the times >40 cycles (data not shown).

Immunohistochemistry

Immunohistochemical staining was performed on 7-µm cryosections PLP-fixed kidney samples. Sections were

Table 1. Sequences of mouse primers used for real-time qPCR[a]

Gene	Forward primer	Reverse primer
GAPDH	5′-TAACATCAAATGGGGTGAGG-3′	5′-GGTTCACACCCATCACAAAC-3′
TRPM6	5′-CCTTGGGGAGTCATTGAGAAC-3′	5′-CAGTCCCATCATCACACAGG-3′
NCC	5′-CTTCGGCCACTGGCATTCTG-3′	5′-GATGGCAAGGTAGGAGATGG-3′
TRPV5	5′-CCACAGTGATGCTGGAGAGG-3′	5′-GGATTCTGCTCCTGGTGGTG-3′
Calbindin-D_{28K}	5′-AACTGACAGAGATGGCCAGGTTA-3′	5′-TGAACTCTTTCCCACACATTTTGAT-3′
PV	5′-CGCTGAGGACATCAAGAAGG-3′	5′-CCGGGTTCTTTTTCTTCAGG-3′
CLDN7	5′-GGATTGGTCATCAGATTGTCACA-3′	5′-TGGCAGGTCCAAACTCGTACT-3′
CLDN8	5′-CATGCCTCAGTGGAGAGTG-3′	5′-GACCTTGCACTGCATTCTG-3′
ENaC	5′-CATGCCTGGAGTCAACAATG-3′	5′-CCATAAAAGCAGGCTCATCC-3′
NHE3	5′-TGCCTTGGTGGTACTTCTGG-3′	5′-TCGCTCCTCTTCACCTTCAG-3′

[a]Mouse primers used to perform SYBR Green real-time quantitative PCR. GAPDH, glyceraldehyde 3-phosphate dehydrogenase; TRPM6, transient receptor potential melastatin member 6; NCC, Na^+, Cl^- cotransporter; TRPV5, transient receptor potential vanilloid member 5; Calbindin-D_{28K}, Ca^{2+}-binding protein D_{28K}; PV, parvalbumin; CLDN7, claudin-7; CLDN8, claudin-8; ENaC, epithelial Na^+ channel; NHE3, Na^+, H^+ exchanger 3.

Table 2. Serum electrolyte concentrations and urine analysis of mice following chronic furosemide treatment[a]

Measurement	Control	Furosemide
Serum		
$[Mg^{2+}]$ (mmol/L)	1.65 ± 0.03	1.57 ± 0.04
$[Ca^{2+}]$ (mmol/L)	2.25 ± 0.04	2.27 ± 0.02
$[Na^+]$ (mmol/L)	147 ± 1	158 ± 3[b]
$[K^+]$ (mmol/L)	7.7 ± 0.1	8.5 ± 0.4
Urine		
Volume (mL/24 h)	1.3 ± 0.2	2.1 ± 0.3[b]
Mg^{2+} excretion (μmol/24 h)	33 ± 3	36 ± 4
Ca^{2+} excretion (μmol/24 h)	7.1 ± 0.7	8.9 ± 0.7
Na^+ excretion (μmol/24 h)	165 ± 12	194 ± 16
K^+ excretion (μmol/24 h)	435 ± 34	490 ± 25

[a]Controls, mice receiving vehicle only; Furosemide, mice receiving 30 mg/kg/day furosemide. Values are presented as mean ± SEM.
[b]$P < 0.05$ compared with control.

stained with guinea pig anti-TRPV5 [25], rabbit anti–calbindin-D_{28K} (Swant, Bellinzona, Switzerland) and rabbit anti-NCC [26], as described previously [27, 28]. Images representing the entire kidney cortex were made using a Zeiss fluorescence microscope (Sliedrecht, the Netherlands) equipped with an AxioCam digital photo camera. For semi-quantitative determination of protein levels as the mean of integrated optical density [28], images were analysed with the Fiji ImageJ image analysis software (http://pacific.mpi-cbg.de).

Immunoblotting

Kidneys of control and furosemide-treated mice were homogenized in homogenization buffer A (HbA; 20 mmol/L Tris/HCl (pH = 7.4), 5 mmol/L $MgCl_2$, 5 mmol/L NaH_2PO_4, 1 mmol/L EDTA, 80 mmol/L sucrose, 1 mmol/L phenylmethanesulfonylfluoride, 1 μg/mL leupeptin and 10 μg/mL pepstatin). Protein concentration of the homogenates was determined using the Bio-Rad Protein Assay (Bio-Rad, Munich, Germany). The proteins were solubilized by 30 min incubation at 37°C in Laemmli buffer. Sixty micrograms of each protein sample were separated on an SDS–PAGE gel and blotted to a polyvinylidene difluoride–nitrocellulose membrane (Immobilon-P, Millipore Corporation, Bedford, MA, USA). Blots were incubated for 16 h with either a rabbit NCC antibody (1:500 dilution; Millipore, Billerica, MA, USA), a rabbit anti–calbindin-D_{28K} (1:10 000 dilution; Swant, Bellinzona, Switzerland), a rabbit anti-αENaC antibody (1:1000 dilution; StressMarq, Victoria, Canada) or a mouse tubulin antibody (1:20 000 dilution; Invitrogen, Camarillo, CA, USA). Thereafter, blots were incubated with peroxidase-conjugated secondary antibodies after which proteins were visualized by chemiluminescence (Pierce, Rockford, IL, USA). Immunopositive bands were scanned using ChemiDoc XRS (Bio-Rad) and signals were analysed with the Quantity One software (Bio-Rad). The amount of NCC, calbindin-D_{28K} and ENaC protein was normalized for the corresponding total amount of protein, using tubulin protein levels or Coomassie staining. Data are based on two independent experiments in which four samples per group were analysed.

Statistical analysis

Data are expressed as mean ± SEM. Statistical analyses were performed by Student's *t*-test. $P < 0.05$ was considered statistically significant. All calculations were accomplished using the InStat 3 for Macintosh software.

Results

Serum and urine electrolyte levels of furosemide-treated mice

Ten-week-old C57Bl/6J mice were administered furosemide or vehicle using osmotic minipumps for 7 days. Before and after the treatment, the mice were individually housed in metabolic cages enabling 24 h urine collections and to measure their water and food intake. Urinary volume and serum electrolyte concentrations and urinary electrolyte levels are displayed in Table 2. The mice treated with furosemide displayed a significant polyuria when compared with controls (2.1 ± 0.3 and 1.3 ± 0.2 mL/24 h respectively, $P < 0.05$). Serum determinations showed that furosemide treatment resulted in substantially increased levels of Na^+ [158 ± 3 (furosemide) and 147 ± 1 mmol/L (control), $P < 0.01$] whereas serum Ca^{2+}, Mg^{2+} and K^+ values were not significantly altered in mice treated with furosemide. Moreover, furosemide treatment did not affect the urinary Mg^{2+}, Ca^{2+}, Na^+ and K^+ excretion (μmol/24 h). Body weight, food intake, water intake and production of faeces were not significantly influenced by the chronic furosemide treatment.

Effect of furosemide treatment on renal expression of TRPM6 and NCC

The effect of furosemide treatment on the renal expression level of TRPM6 was determined by real-time quantitative PCR (qPCR). A significant increase in renal TRPM6 mRNA expression was observed in mice chronically treated with furosemide (129 ± 9 and 100 ± 6%, furosemide versus control, $P < 0.05$) (Figure 1). Next, the renal mRNA expression level and protein abundance of the thiazide-sensitive NCC were determined. Chronic furosemide treatment had no effect on mRNA expression of NCC (98 ± 4 and 100 ± 5%, furosemide versus control, $P > 0.2$) (Figure 2A). The renal protein abundance of NCC was examined by IHC. In order to semi-quantify the protein expression, the amount of immunopositive tubules in the total kidney cortex was determined for each experimental group. The averaged values of the furosemide-treated group are presented as relative percentage of expression in control mice. In contrast with the mRNA level, the protein abundance of NCC was substantially increased (176 ± 9 and 100 ± 8%, furosemide versus control, $P < 0.01$) (Figure 2B).

Specificity of increased levels of Mg^{2+} transporters in response to furosemide administration

To determine the specificity of the upregulation of TRPM6 and NCC in response to furosemide treatment, renal mRNA expression levels of other genes specifically expressed in the DCT and CNT were quantified. To evaluate the effect of furosemide treatment on Ca^{2+} handling, renal expression levels of TRPV5 and the cytosolic Ca^{2+}-binding protein calbindin-D_{28K} in the late DCT (DCT2) and CNT were determined. Furosemide significantly increased the mRNA expression levels of TRPV5 (125 ± 6 and 100 ± 6%, furosemide versus control, $P < 0.01$) (Figure 3A) and calbindin-D_{28K} (153 ± 14 and 100 ± 10%, furosemide versus control, $P < 0.01$) (Figure 3B). Subsequently, the renal protein abundance of TRPV5 and calbindin-D_{28K} was examined by IHC. In accordance with the mRNA levels, the protein levels of TRPV5 (171 ± 18 and 100 ± 10%, furosemide versus control, $P < 0.01$) (Figure 3C) and calbindin-D_{28K} (173 ± 13 and 100 ± 8%, furosemide versus control, $P < 0.01$) (Figure 3D) were markedly increased. Subsequently, the mRNA abundance of parvalbumin (PV), a DCT-specific Ca^{2+}- and Mg^{2+}-binding protein [29], the tight junction proteins claudin-7 (CLDN7) and claudin-8 (CLDN8) expressed along the entire aldosterone-sensitive part of the nephron [30] and the epithelial Na^+ channel (ENaC) in the CNT and collecting duct (CD) were determined by real-time qPCR. Furosemide treatment had no significant effect on the mRNA expression levels of these genes; PV (122 ± 9 and 100 ± 8%) (Figure 4A), CLDN7 (115 ± 6 and 100 ± 11%) (Figure 4B), CLDN8 (103 ± 9 and 100 ± 8%) (Figure 4C) and ENaC (122 ± 13 and 100 ± 7%) (Figure 4D), for all four of these genes; furosemide versus control, $P > 0.05$. Finally, the mRNA expression level of the Na^+–H^+ exchanger 3 (NHE3) in the proximal tubule (PT) and to a minor extent in TAL [31, 32] was determined to define whether chronic furosemide treatment increased Na^+ reabsorption in the PT. Furosemide treatment did not substantially change the renal mRNA level of NHE3 (125 ± 17 and 100 ± 6%, furosemide versus control, $P > 0.1$) (Figure 4E).

Ultimately, to confirm our data obtained by real-time qPCR and IHC, we performed immunoblotting for NCC, calbindin-D_{28K} and αENaC. Quantification of the immunoblots revealed that NCC (165 ± 15 and 100 ± 10%, furosemide versus control, $P < 0.01$) (Figure 5A) and calbindin-D_{28K} (180 ± 23 and 100 ± 12%, furosemide versus control, $P < 0.01$) (Figure 5B) were markedly upregulated in the furosemide-treated group, confirming the results obtained using IHC. Moreover, the immunoblot for ENaC further substantiated the result obtained on the mRNA level, showing that αENaC protein expression is not affected by furosemide treatment as well (122 ± 17 and 100 ± 14%, furosemide versus control, $P > 0.2$) (Figure 5C).

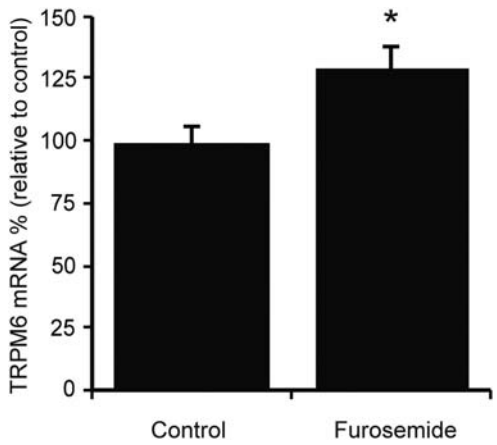

Fig. 1. Effect of chronic furosemide treatment on renal TRPM6 mRNA expression level. Real-time qPCR was used to determine the epithelial Mg^{2+} channel TRPM6 mRNA expression level in the kidneys of mice chronically treated with furosemide (30 mg/kg/day for 7 days). Expression levels are corrected for GAPDH and presented as relative percentage of expression in control mice. Values are presented as means ± SEM ($n = 10$). *$P < 0.05$ compared with control.

Discussion

Our study demonstrated that chronic furosemide treatment induces a robust polyuria. This effect, which is well known for blocking NKCC2, is the consequence of a defect in the urinary concentrating process due to diminished Na^+, K^+ and Cl^- cotransport in the TAL. Importantly, serum Na^+ values were significantly increased, whereas serum Mg^{2+}, Ca^{2+} and K^+ levels remained constant. The renal excretion of these electrolytes was not affected by chronic furosemide administration. Apparently, the abolished reabsorption in the TAL during chronic furosemide treatment is compensated by an enhanced transport of Mg^{2+} and Na^+ in the DCT and of Ca^{2+} in the DCT2 and CNT, via TRPM6, NCC and TRPV5, respectively. These findings demonstrate a large adaptive capacity of the distal part of the nephron during a chronic diuretic regime.

Our furosemide-treated mice did not develop significant hypokalaemia, hypercalciuria or renal K^+ wasting as usually observed for patients treated with furosemide or affected by Bartter syndrome [33, 34]. In contrast, we observed hypernatraemia in the furosemide-treated group. Dehydration is a well-recognized characteristic of Bartter syndrome [34]. Besides, in a mouse model of Bartter syndrome, it was shown that these mice suffer from uncompensated polyuria reflected by extracellular volume depletion and hypernatraemia [35]. Our data suggest that the significant difference in urinary volume was balanced by a smaller, and therefore not significant,

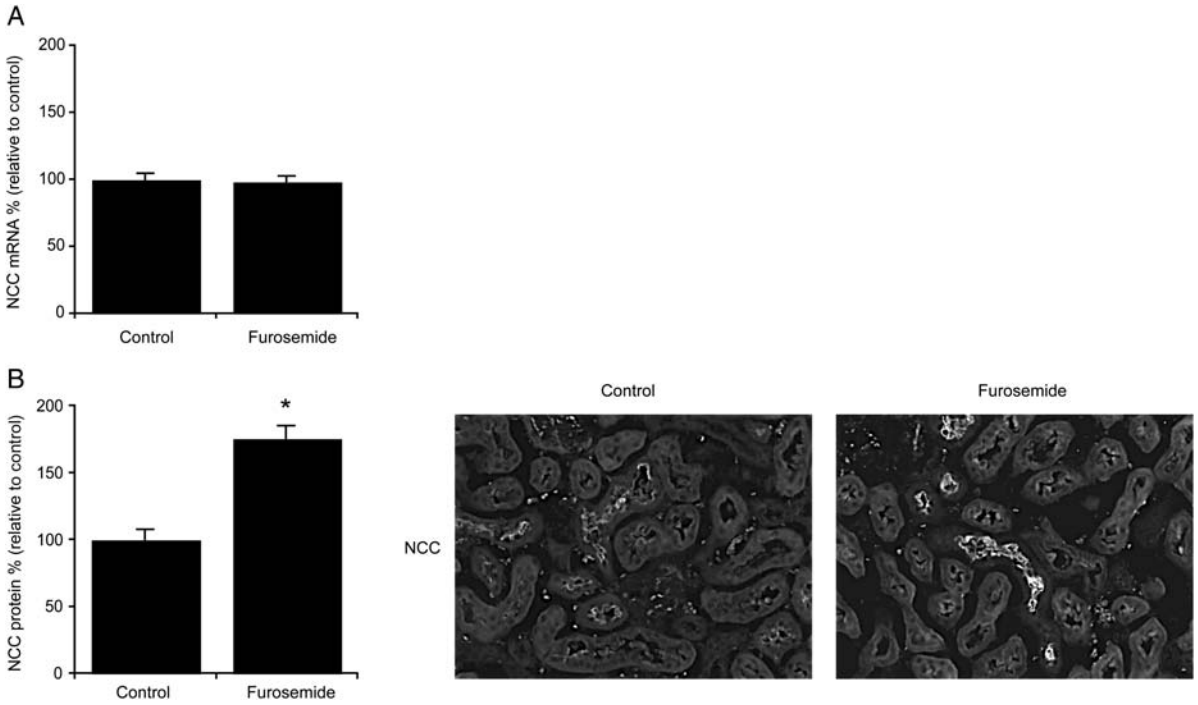

Fig. 2. Effect of chronic furosemide treatment on renal NCC expression levels. Real-time quantitative PCR was used to determine the mRNA level of the thiazide-dependent Na^+, Cl^- cotransporter (NCC) in the kidneys of mice chronically treated with furosemide (30 mg/kg/day for 7 days). Expression levels are corrected for GAPDH and presented as relative percentage of expression in control mice (**A**). NCC protein abundance was determined by computerized analysis of immunohistochemical images and presented as relative percentage of control mice (**B**). Values are presented as means ± SEM ($n = 10$). *$P < 0.05$ compared with control.

compound changes in faeces, water intake and body weight. Consequently, the hypernatraemia probably reflects a loss of water in the furosemide group. Importantly, this could have affected the other electrolyte levels as well. Likewise, NCC-deficient mice appear almost normal since no hypokalaemia was observed and just a mild form of Gitelman syndrome (GS) [36]. This latter finding is unanticipated as well and could indicate that in some cases the mouse is not an optimal model for the human situation.

Our study demonstrated increased mRNA expression level of TRPM6 in response to chronic furosemide treatment. This novel finding unraveled increased active reabsorption of Mg^{2+} in the DCT as a responsible molecular mechanism for the compensation of impaired Mg^{2+} reabsorption in the TAL. The upregulation of TRPM6 in this study demonstrates, as shown before during dietary Mg^{2+} deprivation [37], the gatekeeper function of this channel in the maintenance of the Mg^{2+} balance. Studies on the effect of chronic furosemide application on Mg^{2+} homeostasis are scarce. A minor but significant drop (0.95 ± 0.01 and 0.99 ± 0.01 mmol/L, furosemide versus control, respectively) in plasma Mg^{2+} was found in rats treated with furosemide for several months [38]. In healthy volunteers, oral administration of torasemide (an analogue of furosemide) for 3 weeks did not modify total plasma Mg^{2+}, plasma ionized Mg^{2+} or the free-Mg^{2+} fraction [39]. The sufficient intake of Mg^{2+} during furosemide treatment seems to be fundamental to optimal compensation [9] and aberrations in Mg^{2+} balance probably occur only due to comorbidity [11, 12].

NCC facilitates cotransport of Na^+ and Cl^- into DCT cells. Mutations in the gene encoding NCC cause GS, a salt-losing disorder characterized by hypokalaemic metabolic alkalosis, hypomagnesaemia and hypocalciuria [36, 40]. Moreover, NCC-deficient mice have a similar phenotype, including hypomagnesaemia [36, 40, 41]. This indicates the importance of NCC for Mg^{2+} homeostasis, although it might be an indirect effect since it was not proven that decreased Mg^{2+} reabsorption in TAL is a direct stimulus for upregulation of NCC.

Next, the expression levels of the Ca^{2+} transporter TRPV5 and calbindin-D_{28K}, which are expressed in DCT2 and CNT, were determined. TRPV5 constitutes the apical entry step in active Ca^{2+} reabsorption and is a key player in determining the final urinary Ca^{2+} concentration [42]. TRPV5 and calbindin-D_{28K} were on mRNA as well as on the protein level substantially upregulated, which suggests that like Mg^{2+} transport also active Ca^{2+} transport in the distal part of the nephron is increased upon chronic administration of furosemide. Our results are consistent with the results of Lee *et al.*, concerning the compensatory adaptation of Ca^{2+} reabsorption mediated by an increase in Ca^{2+} transporter abundance in the kidney during chronic furosemide treatment. In contrast with our results obtained after 7 days of treatment, they observed increased urinary excretion of Ca^{2+} after 3 days of furosemide [10]. This apparent discrepancy suggests that the adaptation of the DCT/CNT to chronic furosemide treatment takes more than 3 days to fully compensate for decreased Ca^{2+} reabsorption in the TAL.

Previous studies performed in rats have demonstrated that 6–8 days of continuous furosemide infusion causes hypertrophy of the DCT, CNT and principal cells of the CD [16, 17]. Microperfusion experiments in rats have shown an enhanced capacity for Na^+ reabsorption and K^+

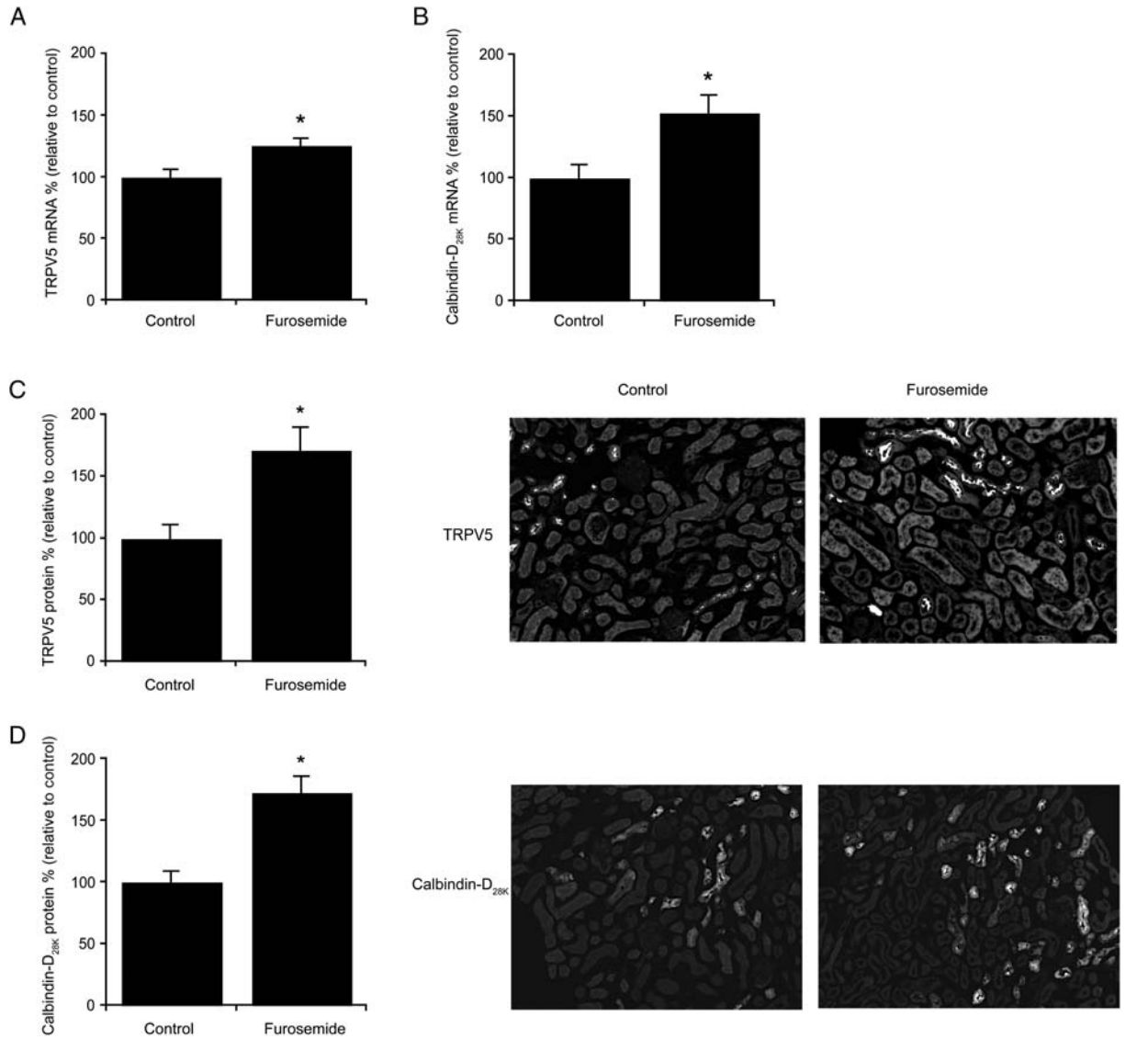

Fig. 3. Effect of chronic furosemide treatment on renal TRPV5 and calbindin-D_{28K} expression levels. Real-time qPCR was used to determine the mRNA expression levels of the epithelial Ca^{2+} channel TRPV5 (**A**) and the cytosolic Ca^{2+}-binding protein calbindin-D_{28K} (**B**) in the kidneys of mice chronically treated with furosemide (30 mg/kg/day for 7 days). Expression levels are corrected for GAPDH and presented as relative percentage of expression in control mice. TRPV5 and calbindin-D_{28K} protein abundance were determined by computerized analysis of immunohistochemical images and presented as relative percentage of control mice (**C** and **D**). Values are presented as means ± SEM ($n = 10$). *$P < 0.05$ compared with control.

secretion by the DCT, CNT and initial CD (ICD) in this adapted state. Furosemide treatment did not affect the length of these tubule segments, but the fractional volumes of the DCT, CNT and ICD were increased, since these cells have increased the height of lateral cell processes and larger nuclei [16]. In the study by Ellison and co-workers, the effect of furosemide was more dramatic, concerning urinary volume, Na^+ excretion and weight loss of the rats compared with our study. This is probably caused by the higher concentration of furosemide used in the former study. We cannot exclude which part/percentage of the compensated reabsorption observed in our study is caused by increased cell volume of the DCT and CNT. However, our results suggest that specific upregulation of TRPM6, NCC and the Ca^{2+} transporters TRPV5 and calbindin-D_{28K} contributes to the increased reabsorption. Additionally, the mRNA expression levels of PV, CLDN7, CLDN8, ENaC and NHE3, as well as the protein level of ENaC were not affected by furosemide treatment. This suggests that the response of the above-mentioned Ca^{2+} and Mg^{2+} transport proteins is rather specific.

In line with our findings, Dussol and co-workers observed in patients that furosemide treatment for 1 month did not significantly increase urinary Na^+ excretion [14, 43]. Loon *et al.* showed that continued renal Na^+ loss during furosemide treatment, also for 1 month and in patients, could be prevented. This was mediated by increased renal Na^+ reabsorption and by a decreased natriuretic response to furosemide [15]. They explained their findings by the negative impact of both the rebound and the braking phenomena. In contrast with those studies where they used once-daily injections, we used osmotic minipumps resulting in continuous release of furosemide. Our procedure makes the occurrence of a

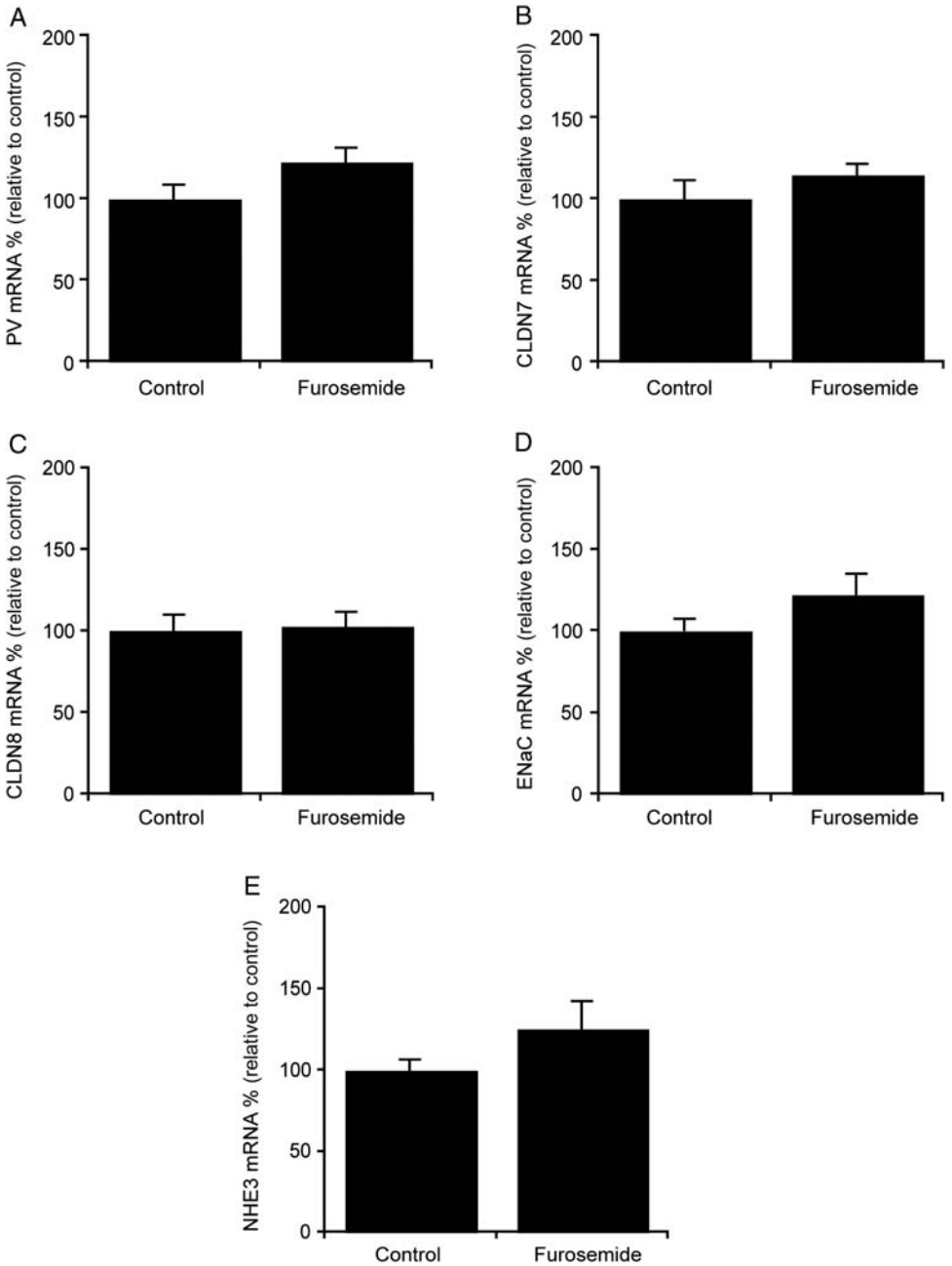

Fig. 4. Effect of chronic furosemide treatment on renal PV, CLDN7, CLDN8, ENaC and NHE3 mRNA expression levels. Real-time qPCR was used to determine mRNA levels of parvalbumin (PV) (**A**), claudin-7 (CLDN7) (**B**), claudin-8 (CLDN8) (**C**), the epithelial Na^+ channel (ENaC) (**D**) and the Na^+–H^+ exchanger 3 (NHE3) (**E**) in the kidneys of mice chronically treated with furosemide (30 mg/kg/day for 7 days). Expression levels are corrected for GAPDH and presented as relative percentage of expression in control mice. Values are presented as means ± SEM ($n = 10$). *$P < 0.05$ compared with control.

rebound period very unlikely, and thus is the compensation probably exclusively mediated by the braking phenomenon. Remarkably, an experiment in rats comparable with our study showed an almost seven times increased urinary volume and four times increased urinary Na^+ excretion levels. Moreover, they observed increased levels of all thee subunits of ENaC, whereas the NCC protein levels were unchanged upon furosemide treatment [44]. In many other studies, furosemide has been shown to increase the abundance and activity of NCC [16, 45, 46]. Interestingly, northern blot analysis of NCC mRNA demonstrated no significant effect of furosemide, similar to our real-time qPCR results, indicating that NCC is specifically regulated on the protein level [46]. The significantly increased serum levels of Na^+ after chronic furosemide treatment found in our study suggest that the furosemide-treated mice developed net water loss, possibly leading to a hypovolaemic state and activation of the renin–angiotensin–aldosterone system.

van der Lubbe *et al.* [47] recently demonstrated that angiotensin II, independently of aldosterone, can increase the abundance and phosphorylation of NCC. This effect is probably mediated in a with-no-lysine kinase (WNK)4-STE20/SPS1-related, proline alanine-rich kinase

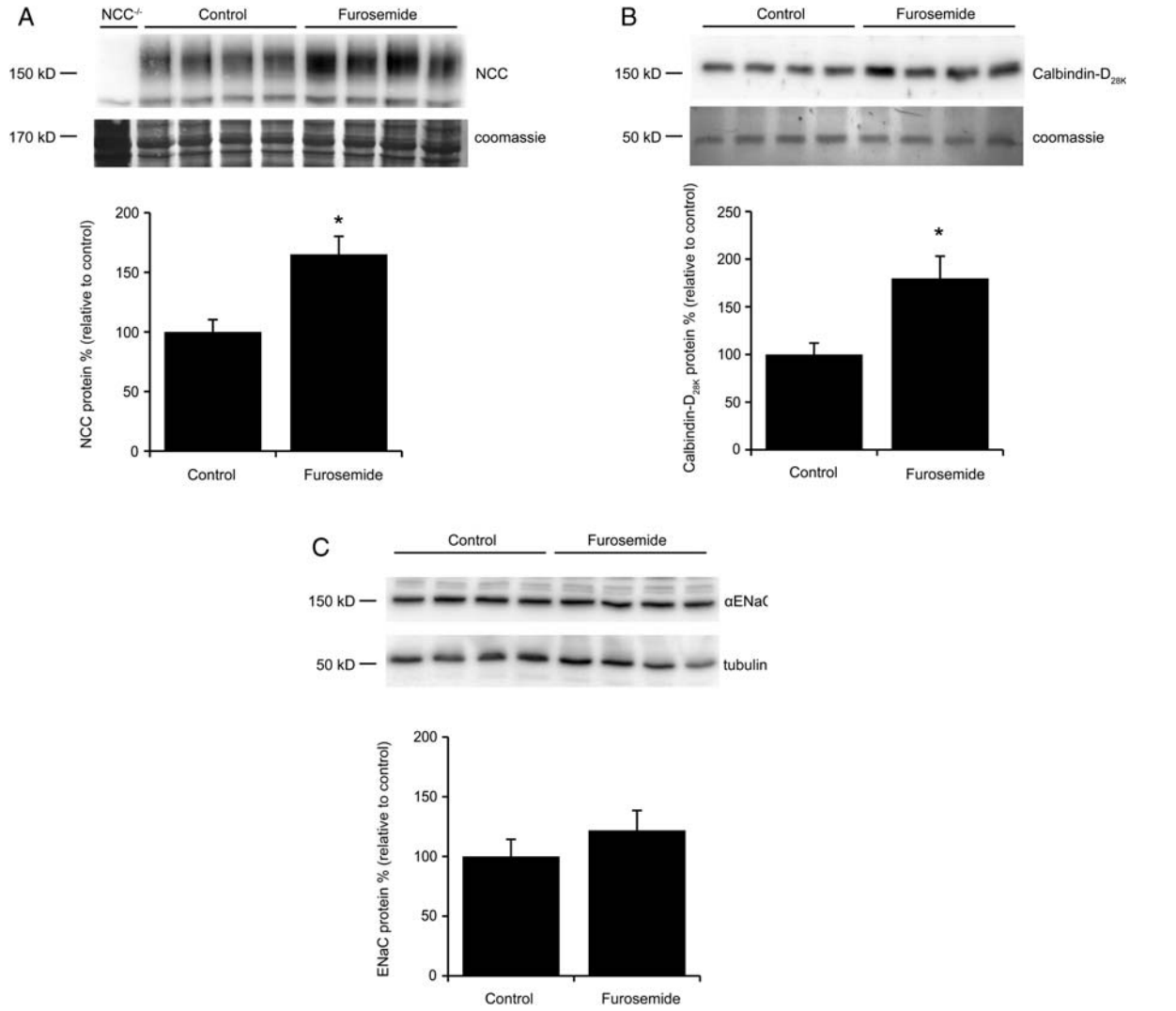

Fig. 5. Effect of chronic furosemide treatment on renal NCC, calbindin-D_{28K} and αENaC protein expression levels. The effect of furosemide (30 mg/kg/day for 7 days) on protein expression levels of the Na^+–Cl^- cotransporter (NCC) (**A**), calbindin-D_{28K} (**B**) and the alpha-subunit of the epithelial Na^+ channel (αENaC) (**C**), determined by immunoblotting. The upper part of each figure shows the immunoblot, with on the left side the molecular mass (in kDa) and the lower parts depict the expression levels as percentage of control. Values are presented as average ± SEM ($n = 4$), while experiments are performed in duplo. *$P < 0.05$ compared with control.

(SPAK)-dependent manner [48]. Specific activation of NCC, as measured in the present study, is a likely explanation for the fact that we did not observe compensated Na^+ reabsorption in the PT via NHE3 as shown for chronic thiazide treatment [26] or stimulation of ENaC in the CNT and CD. Finally, we could not exclude that increased phosphorylation of NCC is mediated by arginine vasopressin, the hormone that primarily serves to control extracellular fluid homeostasis, via the WNK-SPAK/OSR1 pathway [49, 50].

In summary, this study showed that mice adapt to chronic furosemide treatment, by the upregulation of transporters distal to the furosemide target segment, including TRPM6, NCC and TRPV5. In this way, urinary wasting of especially Mg^{2+} and the subsequent development of hypomagnesaemia is prevented. Extrapolating these findings to patients on continuous furosemide treatment, with normal kidney function and consuming an adequate diet, suggests that it is unlikely that they develop hypomagnesaemia. Intriguing remains why patients with mutations in CLDN16 and CLDN19, tight junction proteins located in the TAL, develop hypomagnesaemia due to progressive renal Mg^{2+} wasting [51, 52], while blockade of NKCC2 does not result in hypomagnesaemia. It might be that the effect of mutations in CLDN16 and CLDN19 is more effective compared with blocking NKCC2 by furosemide. Another possible explanation is that CLDN16 and CLDN19 are expressed in more segments than only the TAL.

Funding. This research was financially supported by the Dutch Organization for Scientific Research (ZonMw 9120.8026; ALW 818.02.001), a European Young Investigator award from the European Science Foundation.

Conflict of interest statement. None declared.

References

1. Hendry BM, Ellory JC. Molecular sites for diuretic action. *Trends Pharmacol Sci* 1988; 9: 416–421

2. Rose BD. Diuretics. *Kidney Int* 1991; 39: 336–352
3. Quamme GA. Renal handling of magnesium: drug and hormone interactions. *Magnesium* 1986; 5: 248–272
4. Dimke H, Hoenderop JG, Bindels RJ. Hereditary tubular transport disorders: implications for renal handling of Ca^{2+} and Mg^{2+}. *Clin Sci (Lond)* 2009; 118: 1–18
5. Ellison DH. Diuretic drugs and the treatment of edema: from clinic to bench and back again. *Am J Kidney Dis* 1994; 23: 623–643
6. Di Stefano A, Roinel N, de Rouffignac C *et al*. Transepithelial Ca^{2+} and Mg^{2+} transport in the cortical thick ascending limb of Henle's loop of the mouse is a voltage-dependent process. *Ren Physiol Biochem* 1993; 16: 157–166
7. Quamme GA. Effect of furosemide on calcium and magnesium transport in the rat nephron. *Am J Physiol* 1981; 241: F340–F347
8. Lee AJ, Chen YH, Chu ML *et al*. [Effect of furosemide on renal magnesium and calcium excretion of different ages (II)]. *Zhonghua Min Guo Xiao Er Ke Yi Xue Hui Za Zhi* 1994; 35: 215–220
9. Caddell JL. Protection by magnesium of renal calcinosis in furosemide-treated weanling rats with moderate magnesium deficiency. *Biol Neonate* 1985; 48: 49–58
10. Lee CT, Chen HC, Lai LW *et al*. Effects of furosemide on renal calcium handling. *Am J Physiol Renal Physiol* 2007; 293: F1231–7
11. Cohen N, Almoznino-Sarafian D, Zaidenstein R *et al*. Serum magnesium aberrations in furosemide (frusemide) treated patients with congestive heart failure: pathophysiological correlates and prognostic evaluation. *Heart* 2003; 89: 411–416
12. Davies DL, Fraser R. Do diuretics cause magnesium deficiency? *Br J Clin Pharmacol* 1993; 36: 1–10
13. Jentzer JC, DeWald TA, Hernandez AF. Combination of loop diuretics with thiazide-type diuretics in heart failure. *J Am Coll Cardiol* 2010; 56: 1527–1534
14. Ellison DH. The physiologic basis of diuretic synergism: its role in treating diuretic resistance. *Ann Intern Med* 1991; 114: 886–894
15. Loon NR, Wilcox CS, Unwin RJ. Mechanism of impaired natriuretic response to furosemide during prolonged therapy. *Kidney Int* 1989; 36: 682–689
16. Ellison DH, Velazquez H, Wright FS. Adaptation of the distal convoluted tubule of the rat. Structural and functional effects of dietary salt intake and chronic diuretic infusion. *J Clin Invest* 1989; 83: 113–126
17. Kaissling B, Bachmann S, Kriz W. Structural adaptation of the distal convoluted tubule to prolonged furosemide treatment. *Am J Physiol* 1985; 248: F374–F381
18. Branch RA, Homeida M, Levine D *et al*. Pharmacokinetics of frusemide related to diuretic response [proceedings]. *Br J Pharmacol* 1976; 57: 442P–443P
19. Andreasen F, Lauridsen IN, Hansen FA *et al*. Dose dependency of furosemide-induced sodium excretion. *J Pharmacol Exp Ther* 1989; 248: 1182–1188
20. Schlingmann KP, Konrad M, Seyberth HW. Genetics of hereditary disorders of magnesium homeostasis. *Pediatr Nephrol* 2004; 19: 13–25
21. Simon DB, Karet FE, Hamdan JM *et al*. Bartter's syndrome, hypokalaemic alkalosis with hypercalciuria, is caused by mutations in the Na-K-2Cl cotransporter NKCC2. *Nat Genet* 1996; 13: 183–188
22. Voets T, Nilius B, Hoefs S *et al*. TRPM6 forms the Mg2+ influx channel involved in intestinal and renal Mg2+ absorption. *J Biol Chem* 2004; 279: 19–25
23. Bachmann S, Velazquez H, Obermuller N *et al*. Expression of the thiazide-sensitive Na-Cl cotransporter by rabbit distal convoluted tubule cells. *J Clin Invest* 1995; 96: 2510–2514
24. Hoenderop JG, Muller D, Van Der Kemp AW *et al*. Calcitriol controls the epithelial calcium channel in kidney. *J Am Soc Nephrol* 2001; 12: 1342–1349
25. Hoenderop JG, Hartog A, Stuiver M *et al*. Localization of the epithelial Ca^{2+} channel in rabbit kidney and intestine. *J Am Soc Nephrol* 2000; 11: 1171–1178
26. Nijenhuis T, Hoenderop JG, Loffing J *et al*. Thiazide-induced hypocalciuria is accompanied by a decreased expression of Ca^{2+} transport proteins in kidney. *Kidney Int* 2003; 64: 555–564
27. Hoenderop JG, van Leeuwen JP, van der Eerden BC *et al*. Renal Ca^{2+} wasting, hyperabsorption, and reduced bone thickness in mice lacking TRPV5. *J Clin Invest* 2003; 112: 1906–1914
28. Nijenhuis T, Hoenderop JG, Bindels RJ. Downregulation of Ca (2+) and Mg(2+) transport proteins in the kidney explains tacrolimus (FK506)-induced hypercalciuria and hypomagnesaemia. *J Am Soc Nephrol* 2004; 15: 549–557
29. Bindels RJ, Timmermans JA, Hartog A *et al*. Calbindin-D9k and parvalbumin are exclusively located along basolateral membranes in rat distal nephron. *J Am Soc Nephrol* 1991; 2: 1122–1129
30. Li WY, Huey CL, Yu AS. Expression of claudin-7 and -8 along the mouse nephron. *Am J Physiol Renal Physiol* 2004; 286: F1063–F1071
31. Amemiya M, Loffing J, Lotscher M *et al*. Expression of NHE-3 in the apical membrane of rat renal proximal tubule and thick ascending limb. *Kidney Int* 1995; 48: 1206–1215
32. Nishinaga H, Komatsu R, Doi M *et al*. Circadian expression of the Na^+/H^+ exchanger NHE3 in the mouse renal medulla. *Biomed Res* 2009; 30: 87–93
33. Suki WN, Eknoyan G, Martinez-Maldonado M. Tubular sites and mechanisms of diuretic action. *Annu Rev Pharmacol* 1973; 13: 91–106
34. Bartter FC, Pronove P, Gill JR Jr. *et al*. Hyperplasia of the juxtaglomerular complex with hyperaldosteronism and hypokalemic alkalosis. A new syndrome. *Am J Med* 1962; 33: 811–828
35. Takahashi N, Chernavvsky DR, Gomez RA *et al*. Uncompensated polyuria in a mouse model of Bartter's syndrome. *Proc Natl Acad Sci USA* 2000; 97: 5434–5439
36. Schultheis PJ, Lorenz JN, Meneton P *et al*. Phenotype resembling Gitelman's syndrome in mice lacking the apical Na+-Cl-cotransporter of the distal convoluted tubule. *J Biol Chem* 1998; 273: 29150–5
37. Groenestege WM, Hoenderop JG, van den Heuvel L *et al*. The epithelial Mg^{2+} channel transient receptor potential melastatin 6 is regulated by dietary Mg2+ content and estrogens. *J Am Soc Nephrol* 2006; 17: 1035–1043
38. Wong NL, Sutton RA, Dirks JH. Is lymphocyte magnesium concentration a reflection of intracellular magnesium concentration? *J Lab Clin Med* 1988; 112: 721–726
39. Gozzi T, Durler S, Truttman AC *et al*. Free circulating magnesium and loop diuretics in humans. *Eur J Clin Pharmacol* 1997; 53: 275–276
40. Simon DB, Nelson-Williams C, Bia MJ *et al*. Gitelman's variant of Bartter's syndrome, inherited hypokalaemic alkalosis, is caused by mutations in the thiazide-sensitive Na-Cl cotransporter. *Nat Genet* 1996; 12: 24–30
41. Gitelman HJ, Graham JB, Welt LG. A new familial disorder characterized by hypokalemia and hypomagnesaemia. *Trans Assoc Am Physicians* 1966; 79: 221–235
42. Hoenderop JG, van der Kemp AW, Hartog A *et al*. Molecular identification of the apical Ca^{2+} channel in 1,25-dihydroxyvitamin D3-responsive epithelia. *J Biol Chem* 1999; 274: 8375–8378
43. Dussol B, Moussi-Frances J, Morange S *et al*. A randomized trial of furosemide vs hydrochlorothiazide in patients with chronic renal failure and hypertension. *Nephrol Dial Transplant* 2005; 20: 349–353

44. Na KY, Oh YK, Han JS *et al*. Upregulation of Na^+ transporter abundances in response to chronic thiazide or loop diuretic treatment in rats. *Am J Physiol Renal Physiol* 2003; 284: F133–F143
45. Stanton BA, Kaissling B. Adaptation of distal tubule and collecting duct to increased Na delivery. II. Na^+ and K^+ transport. *Am J Physiol* 1988; 255: F1269–F1275
46. Abdallah JG, Schrier RW, Edelstein C *et al*. Loop diuretic infusion increases thiazide-sensitive Na(+)/Cl(−)-cotransporter abundance: role of aldosterone. *J Am Soc Nephrol* 2001; 12: 1335–1341
47. van der Lubbe N, Lim CH, Fenton RA *et al*. Angiotensin II induces phosphorylation of the thiazide-sensitive sodium chloride cotransporter independent of aldosterone. *Kidney Int* 2011; 79: 66–76
48. San-Cristobal P, Pacheco-Alvarez D, Richardson C *et al*. Angiotensin II signaling increases activity of the renal Na-Cl cotransporter through a WNK4-SPAK-dependent pathway. *Proc Natl Acad Sci USA* 2009; 106: 4384–4389
49. Mutig K, Saritas T, Uchida S *et al*. Short-term stimulation of the thiazide-sensitive Na+–Cl– cotransporter by vasopressin involves phosphorylation and membrane translocation. *Am J Physiol Renal Physiol* 2010; 298: F502–F509
50. Pedersen NB, Hofmeister MV, Rosenbaek LL *et al*. Vasopressin induces phosphorylation of the thiazide-sensitive sodium chloride cotransporter in the distal convoluted tubule. *Kidney Int* 2010; 78: 160–169
51. Simon DB, Lu Y, Choate KA *et al*. Paracellin-1, a renal tight junction protein required for paracellular Mg^{2+} resorption. *Science* 1999; 285: 103–106
52. Konrad M, Schaller A, Seelow D *et al*. Mutations in the tight-junction gene claudin 19 (CLDN19) are associated with renal magnesium wasting, renal failure, and severe ocular involvement. *Am J Hum Genet* 2006; 79: 949–957

Received for publication: 31.1.12; Accepted in revised form: 6.9.12